



**HAL**  
open science

## Using LVIC in current mode for energy spectrum reconstruction: Experiments and validation

D Mazon, D Colette, E Soudet, P Malard, M Walsh, M Moreau, A Jardin

### ► To cite this version:

D Mazon, D Colette, E Soudet, P Malard, M Walsh, et al.. Using LVIC in current mode for energy spectrum reconstruction: Experiments and validation. *Review of Scientific Instruments*, In press. cea-03786722

**HAL Id: cea-03786722**

**<https://cea.hal.science/cea-03786722>**

Submitted on 23 Sep 2022

**HAL** is a multi-disciplinary open access archive for the deposit and dissemination of scientific research documents, whether they are published or not. The documents may come from teaching and research institutions in France or abroad, or from public or private research centers.

L'archive ouverte pluridisciplinaire **HAL**, est destinée au dépôt et à la diffusion de documents scientifiques de niveau recherche, publiés ou non, émanant des établissements d'enseignement et de recherche français ou étrangers, des laboratoires publics ou privés.

# Using LVIC in current mode for energy spectrum reconstruction: Experiments and validation

D. Mazon<sup>1,a)</sup>, D. Colette<sup>2</sup>, E. Soudet<sup>3</sup>, P. Malard<sup>1</sup>, M. Walsh<sup>2</sup>, M. Moreau<sup>1</sup> and A. Jardin<sup>4</sup>

<sup>1</sup>CEA, IRFM, F-13108 Saint-Paul-lez-Durance, France

<sup>2</sup>ITER Organization, Route de Vinon sur Verdon, CS 90 046, 13067, Saint-Paul-lez Durance Cedex, France

<sup>3</sup>ENSI CAEN, 6 boulevard Maréchal Juin, 14000 Caen, France

<sup>4</sup>Institute of Nuclear Physics Polish Academy of Sciences (IFJ PAN), PL-31-342, Krakow, Poland

<sup>a)</sup>Author to whom correspondence should be addressed: [didier.mazon@cea.fr](mailto:didier.mazon@cea.fr).

(Presented XXXXX; received XXXXX; accepted XXXXX; published online XXXXX)

Due to the ITER radiative environment, in particular during high D-T power phase classic X-ray detectors such as semiconductor diodes might be too fragile and are thus not viable. Instead, advanced detectors such as gas-filled detectors are nowadays considered. The Low Voltage Ionization Chamber (LVIC) is one of the most promising candidate for X-ray measurement during the ITER nuclear phase. A complete model of the detector recently developed at IRFM now requires experimental validation. Experimental testing at the IRFM laboratory of an ITER industrial LVIC prototype and comparison with modelling are presented. In particular, an original approach to extract information on the X-ray spectrum from current-mode LVIC measurement is validated experimentally.

## I. INTRODUCTION

### A. Background

In tokamaks with tungsten (W) plasma facing components such as the International Thermonuclear Experimental Reactor (ITER), pollution of the plasma by heavy impurities is a major concern as it can lead to radiative breakdown. A diagnostic allowing reconstruction of the impurity distribution is thus of high interest. The radiation emitted by such impurities is mainly composed of X-rays in the 0.1 - 100 keV range. Due to the ITER radiative environment, in particular during high D-T power phase, classic X-ray detectors such as semiconductor diodes might be too fragile and are thus not viable. Instead, advanced detectors such as gas-filled detectors are nowadays considered. The Low Voltage Ionization Chamber (LVIC) is one of the most promising candidate for X-ray measurement during the ITER nuclear phase [1]. A complete model of the detector recently developed at IRFM [2] now requires experimental validation.

Experimental testing at the IRFM laboratory of an industrial LVIC prototype filled with argon and comparison with modelling are presented. In particular, an original approach [3] to extract information on the X-ray spectrum (and thus indirectly on impurity distribution) from current-mode LVIC measurements is validated. Finally, conclusions are drawn on the potential application to the ITER tokamak.

### B. Low Voltage Ionization Chamber (LVIC)

A schematic representation of the LVIC concept is introduced in Fig. 1, for which X-ray photons are the radiation of interest throughout this paper.

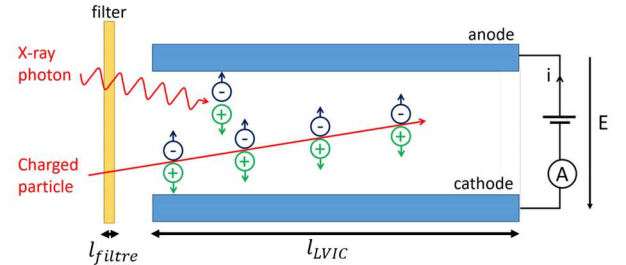


FIG. 1. LVIC schematic representation.

The detection in the LVIC of an incident photon flux  $\phi$  of energy  $h\nu$  is given by:

$$\phi^{det}(h\nu) = T(h\nu) \cdot A(h\nu) \cdot \phi(h\nu) \quad (1)$$

where  $\phi^{det}$  is the detected part of the photon flux,  $T$  is the transmission coefficient through the filter and  $A$  is the coefficient of photoelectric absorption in the gas. The coefficient of transmission  $T$  through the filter is expressed as:

$$T(h\nu) = \exp(-N_m \cdot \sigma_{tot}(h\nu) \cdot l_{\text{filter}}) \quad (2)$$

where  $N_m$  is the density of the material in  $m^{-3}$ ,  $\sigma_{tot}$  is the total cross section in  $m^2$  and  $l_{\text{filter}}$  is the thickness of the filter in  $m$ . The coefficient of photoelectric absorption  $A$  in the gas is expressed as:

$$A(h\nu) = 1 - \exp(-N_g \cdot \sigma_{ph}(h\nu) \cdot l_{LVIC}) \quad (3)$$

where  $N_g$  is the density of the gas in  $m^{-3}$ ,  $\sigma_{ph}$  is the photoionization cross-section in  $m^2$ , and  $l_{LVIC}$  is the length of the ionization chamber in  $m$ . The total cross sections used in this work were extracted from the theoretical XCOM photon cross-sections database developed by the National Institute of Standards and Technology (NIST) [4].

During photoionization of a gas atom by a photon of energy  $h\nu$ , a bound electron is emitted with a kinetic energy  $E_{kin} = h\nu - E_B$ , with  $E_B$  the electron bound energy. The ionized atom can go through de-excitation either by Auger electron emission or by X-ray fluorescence with a given probability  $P_f$ . In the case of X-ray fluorescence (above a threshold  $h\nu > E_X$ ) the lost charge is  $\Delta C_f = E_B/W$ , with  $W$  the mean ionization energy of the gas, leading to the so-called escape peak in the measured spectrum. For argon, the probability  $P_f = 14\%$ ,  $E_X = 3.2 \text{ keV}$ ,  $E_B = 2.9 \text{ keV}$  and  $W = 26 \text{ eV}$  [5]. The statistical fluctuations  $\sigma_N^2$  in the number of charges  $N$  induced by photoionization of the gas are described by:

$$\frac{\sigma_N^2}{\langle N \rangle^2} = \frac{F}{\langle N \rangle} \quad (4)$$

where  $F$  is the so-called Fano factor, which has a value of 0.23 for argon [6].

## II. EXPERIMENTAL SETUP

The experimental setup is introduced in Fig. 2. A soft X-ray (SXR) source SRI SB-50-1k was used, with a beam of accelerated electrons hitting a W target, producing X-ray bremsstrahlung and characteristic W line emission. First, a Si-PIN diode XR-100CR was used as the reference detector and was positioned  $81 \text{ cm}$  away from the source, to acquire the spectrum and characterize the SXR source in the energy range  $1 - 30 \text{ keV}$ . In a second phase, the Si-PIN detector was swapped with the LVIC prototype. Pictures of the Si-PIN diode and of the LVIC prototype, filled here with argon at 1 bar of pressure and with an applied voltage of  $600 \text{ V}$ , are presented in Fig. 3. A set of aluminium filters with a total thickness of up to  $969 \mu\text{m}$  could be placed between the source and the detector, to play the role of a high-pass filter. As depicted in Fig. 4, the aluminium filters practically damp all SXR radiation below  $\sim 10 \text{ keV}$ , while the layer of  $81 \text{ cm}$  of air only cuts the signal below  $\sim 5 \text{ keV}$ .

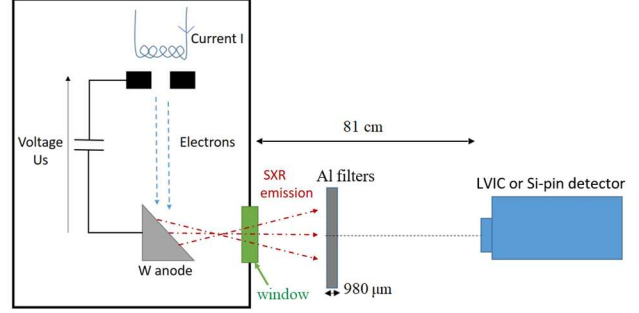


FIG. 2. Experimental setup for SXR generation and measurements.

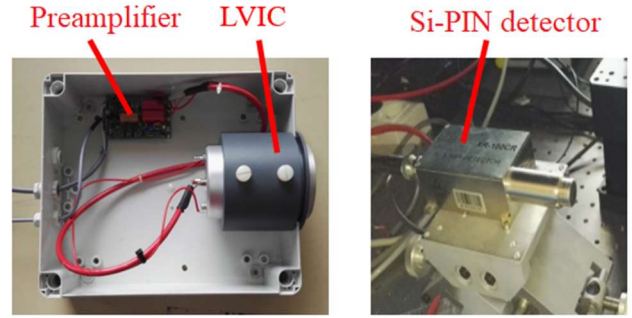


FIG. 3. Left: photo of the LVIC prototype. Right: photo of the Si-pin diode.

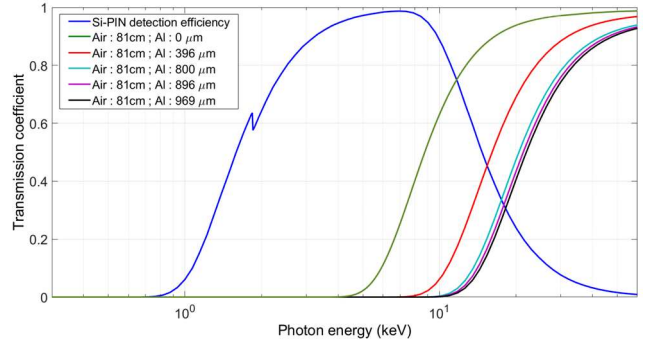


FIG. 4. Transmission coefficients of Si-Pin, air and aluminium widths.

An experimental SXR spectrum acquired by the Si-pin diode for the source parameters  $I = 10 \mu\text{A}$  and  $U_s = 10 \text{ kV}$  is presented in Fig. 4. Two peaks are visible at about  $h\nu_1 \approx 10 \text{ keV}$  and  $h\nu_2 \approx 11.5 \text{ keV}$ , likely corresponding to the W line emission  $L\beta$  ( $9.96 \text{ keV}$ ) and  $L\gamma$  ( $11.42 \text{ keV}$ ). The signal is strongly attenuated for  $h\nu \leq 10 \text{ keV}$  due to absorption by the filters and likely only noise is recorded. For  $20 \text{ keV} \leq h\nu \leq 30 \text{ keV}$ , the spectrum is rather flat with a low intensity close to the noise level. The peak observed at  $30 \text{ keV}$  simply corresponds to the detection limit of the system and is related to the pile-up effect.

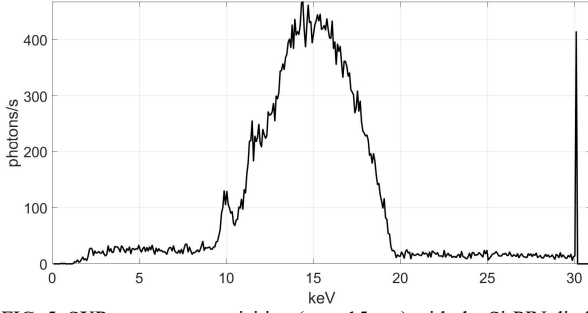


FIG. 5. SXR spectrum acquisition (over 15 sec) with the Si-PIN diode, for aluminium filters of 969  $\mu\text{m}$  thickness and source parameters  $I = 10 \mu\text{A}$  and  $U_s = 10 \text{kV}$ . The peak observed at 30 keV simply corresponds to the detection limit of the Si-PIN and is related to pile-up.

The spatial distribution of the SXR source was also checked, as reported in Fig. 5. The detection area of the Si-PIN ( $7 \text{mm}^2$ ) is represented by the small colorful squares. It can be seen that the source exhibited a relatively good spatial homogeneity inside a radius of 25 - 30 mm from the emission axis (at a distance of 81 cm from the source). The red circle corresponds to the detection area of the LVIC ( $24 \text{cm}^2$ ). The worst deviation is observed in the vertical direction, with a total number of count decreasing from  $4.1 \times 10^4$  to  $3.8 \times 10^4$  (i.e.  $< 10\%$ ) for a vertical shift of 40 mm. This is a satisfactory results given the LVIC dimensions and the source was considered as spatially uniform in this setup.

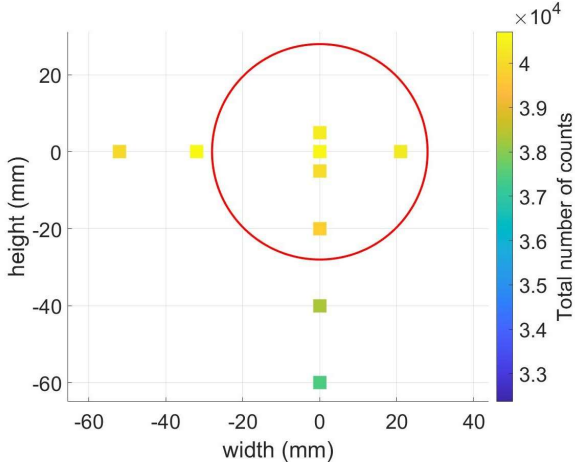


FIG. 6. SXR source spatial distribution measured with the Si-PIN, showing a relatively good homogeneity up to 25 - 30 mm away from the emission axis. The colourful squares correspond to the Si-PIN detection area ( $7 \text{mm}^2$ ) while the red circle denotes the LVIC area ( $24 \text{cm}^2$ ).

### III. METHODOLOGY

#### A. Incident spectrum deconvolution

The purpose of this work was to recover spectral information about the incident photon flux from LVIC measurements in current-mode. The proposed approach is to measure the LVIC current  $I_{meas}$  with different aluminium filter thicknesses, in order to collect information about different parts of the spectrum. It can be noted here that this

simple approach is equivalent to the use of a multi-chamber LVIC for spectrum reconstruction, as discussed in [3]. Such study is therefore a first step to validate the multi-chamber concept.

Since the reconstruction problem is ill-posed, it is proposed to model the incident spectrum  $\phi$  (before absorption by air and Al filters) using a simple mathematical function, defined for  $h\nu < h\nu_{lim}$  by:

$$\phi(h\nu) = X_1 e^{-\frac{(h\nu-h\nu_1)^2}{2\sigma_1^2}} + X_2 e^{-\frac{(h\nu-h\nu_2)^2}{2\sigma_2^2}} + X_3 - X_4 h\nu \quad (5)$$

with a decreasing linear slope to approximate the bremsstrahlung in this energy range and where the values  $h\nu_1 = 9.961 \text{keV}$ ,  $h\nu_2 = 11.42 \text{keV}$ ,  $\sigma_1 = 0.1225 \text{keV}$ ,  $\sigma_2 = 0.2739 \text{keV}$  have been chosen to fit the observed W emission lines with Gaussian functions.  $\{X_1, X_2, X_3, X_4\}$  are unknown parameters to determine. The spectrum is also assumed to be flat at higher energies up to 30 keV, i.e.  $\phi(h\nu_{lim} < h\nu < 30 \text{keV}) = X_5$  and  $\phi(h\nu > 30 \text{keV}) = 0$  with  $h\nu_{lim} = (X_3 - X_5)/X_4$  to ensure continuity of the spectrum at  $h\nu = h\nu_{lim}$ , such that the modelled spectrum is fully determined by a set of five parameters  $\{X_i\}_{i=\llbracket 1..5 \rrbracket}$ . It is therefore necessary to collect at least five LVIC currents with different aluminum filter thicknesses to reconstruct the parametric spectrum. The following available Al thicknesses have been chosen:  $l_{filter} = \{0, 396, 800, 896, 969 \mu\text{m}\}$  as reported in Fig. 4.

The reconstruction of the incident spectrum is achieved thanks to a chi-square minimization procedure:

$$\{X_i\}_{i=\llbracket 1..5 \rrbracket} = \arg \min \|I_{meas} - I_{synt}(\phi(X))\|_2^2 \quad (6)$$

where the strategy is to iteratively optimize the set of parameters  $\{X_i\}_{i=\llbracket 1..5 \rrbracket}$  to minimize the discrepancy between LVIC experimental measurements  $I_{meas}$  and LVIC synthetic measurements  $I_{synt}$  expected from the modelled spectrum.

#### B. LVIC synthetic measurements

The X-ray detection process in the LVIC is modelled using matrix computation as described in [7]. The expected current  $I_{synt}$  that should be collected by the LVIC for a given incident photon flux  $\phi$  is determined by:

$$I_{synt} = e \cdot M_C \cdot M_X \cdot M_A \cdot M_f \cdot \phi \quad (7)$$

where  $M_f$  is the matrix associated to filter transmission and  $M_A$  to photo-electric absorption in the gas,  $M_X$  is the matrix describing the effect of X-ray fluorescence and Auger emission on the photon flux (i.e. including the argon escape peak),  $M_C$  is the matrix associated to charge collection and statistical fluctuations due to the Fano factor and  $e$  denotes

the elementary charge. Further details about the exact expressions of these matrices can be found in [7].

#### IV. RESULTS

In a first step, the capability to simulate the LVIC measurements with the SXR source characterized by the Si-PIN was investigated. For this purpose, the gain of the preamplifier was determined experimentally in an electronic lab. The preamplifier had an estimated gain of  $G \approx 130 M\Omega$ . The measured LVIC voltage could then be compared with the simulated one, after deconvolution of the acquired spectrum  $\phi$  with the Si-PIN response function and the use of Eq. (7). The results are presented in Table 1, with and without the aluminium filters. It is found that the experimental voltage is retrieved in both cases with a relative error of about 5%, validating the simulation procedure.

TABLE I. Experimental results – model validation.

Al filter width ( $\mu\text{m}$ )	Measured voltage (mV)	Simulated voltage (mV)	Relative error (%)
969	7.36	7.71	4.5
0	191.22	203.29	5.9

In a second step, five LVIC measurements were collected with different Al filters thicknesses  $l_{filter} = \{0, 396, 800, 896, 969 \mu\text{m}\}$  in order to reconstruct the parametric spectrum as described in Section III. The chi-square minimization procedure led to the following set of optimized parameters:  $\{X_1, X_2, X_3, X_4, X_5\} = 10^5 \times \{26, 4.1, 7.7, 0.4, 0.045\}$  and therefore  $h\nu_{lim} \approx 19.14 \text{ keV}$ . The parametric spectrum reconstructed in this way (and convolved with air + Al filter transmission coefficients) is presented in Fig. 7, together with the estimated incident spectrum on the LVIC based on the Si-PIN experimental spectrum of Fig. 5 - after deconvolution by the Si-PIN detection efficiency and multiplication by the LVIC over Si-PIN surface ratio  $\sim 343$  (and where the unphysical “pile-up” peak at 30 keV has been cleared out). It can be observed that the incident spectrum is reconstructed in a consistent manner by the Si-PIN and the multi-LVIC measurements with this approach.

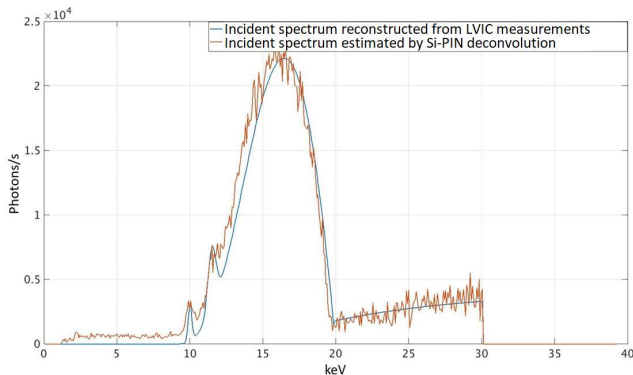


FIG. 7. Estimated incident spectrum on the LVIC entrance window (after air + Al filters), as obtained by the Si-PIN spectrum deconvolution (in orange) and reconstructed with the multi-LVIC measurements (in blue).

#### V. DISCUSSION

In this work, LVIC synthetic modelling has been experimentally validated with a relative error of 5% in the proposed experimental setup relying on an argon-filled LVIC prototype. It has been shown that a discrete set of current measurements associated to chi-square minimization can be used to get spectral information about the incident SXR radiation. In particular, the inversion method developed in [3] has been successfully applied to experimental measurements. This is a first promising result to demonstrate the capability of a multi-chamber LVIC to extract spectral information from a discrete set of measured current, which could be of great interest for ITER and future fusion reactors.

Therefore, the next steps of this work could include the design and construction of a multi-chamber LVIC prototype and its experimental testing in a X-ray laboratory and on a tokamak.

#### ACKNOWLEDGMENTS

The views and opinions expressed in this paper do not necessarily reflect those of the ITER Organization nor those of Fusion for Energy.

#### DATA AVAILABILITY

The data that support the findings of this study are available from the corresponding author upon reasonable request.

#### REFERENCES

- [1] Y.V. Gott, M.M. Stepanenko, “A low-voltage ionization chamber for the ITER”, *Instrum Exp Tech* 52 (2009) 260–264.
- [2] D. Colette et al., “Modeling a low voltage ionization chamber based tomography system on,” *Rev. Sci. Instrum.* 91 (2020) 073504.
- [3] D. Colette et al., “Conceptual study of energy resolved x-ray measurement and electron temperature reconstruction on ITER with low voltage ionization chambers,” *Rev. Sci. Instrum.* 92 (2021) 083511.
- [4] M. J. Berger et al., “XCOM: Photon cross sections database,” *NIST Standard Reference Database 8* (2009) 87-3597.
- [5] T. Watanabe, HW Schnopper and FN Cirillo. “K X-ray fluorescence yield of argon”, *Physical Review* 127.6 (1962), p. 2055.
- [6] A. Hashiba, K. Masuda, T. Doke, T. Takahashi, and Y. Fujita, “Fano factor in gaseous argon measured by the proportional scintillation method,” *Nucl. Instrum. Methods Phys. Res., Sect. A* 227(2) (1984) 305–310.
- [7] D. Colette, “Innovative x-ray diagnostic for impurity transport on ITER. Plasma”, PhD thesis, Aix-Marseille University (2021), HAL Id: tel-03153486.